Polymer Bulletin (2022) 79:5939–5954
https://doi.org/10.1007/s00289-021-03788-6

ORIGINAL PAPER

# GO containing PHBHX bone scaffold: GO concentration and in vitro osteointegration

**Arslan Kağan Arslan[1] · Ekin Çelik[2] · Funda Alkan[3] · Murat Demirbilek[4]**

Received: 4 March 2021 / Revised: 30 May 2021 / Accepted: 8 June 2021 /
Published online: 17 June 2021


## Abstract

Trauma, congenital abnormalities or cancer-induced bone defects can be treated with tissue engineering products. Graphene oxide-containing polymeric scaffolds are used as an artificial extracellular matrix, acting as an environment where cells can grow and turn into living tissues. In the presented study, primarily cytotoxicity of graphene oxide was determined depending on the concentration. According to the cytotoxicity results, two different scaffolds containing low and high concentrations of GO were prepared and usability in bone tissue engineering was examined. For this purpose, water uptake, in vitro degradation and mechanical properties of the scaffolds were determined. On the predetermined days, MC3T3 cells proliferation and ACTB, COL1A1, OCN, OPN, RUNX2 gene expression were determined. According to the results, MC3T3 cell proliferation was increased when the incubation time increased, and also, gene expression related to bone tissue formation was increased.

**Keywords** Cytotoxicity of GO · GO bone · PHBHX bone scaffolds · Osteointegration of scaffolds

✉ Arslan Kağan Arslan
arslankagan2020@gmail.com

[1] Department of Orthopedics and Traumatology, Yenimahalle Education and Research Hospital, Yıldırım Beyazıt University, Ankara, Turkey

[2] Medical Biology Department, Faculty of Medicine, Ahi Evran University, Kırşehir, Turkey

[3] Advanced Technologies Applications and Research Center, Hacettepe University, Ankara, Turkey

[4] Biology Department, Ankara Hacı Bayram Veli University, Ankara, Turkey

## Introduction

Trauma, congenital abnormalities, or cancer-induced bone defects can be treated with tissue engineering products. Polymeric scaffolds are used as an artificial extracellular matrix in tissue engineering, acting as an environment where cells can grow and turn into living tissues [1]. The most important features of the scaffolds are their biocompatibility and biodegradation abilities. The scaffolds should provide support to the proliferating cells and be gradually degraded and absorbed during the process, in which these degradation products should be non-toxic to the surrounding tissue [2]. In addition, the shape and composition of the scaffolds should be compatible with the host tissue [3]. Metals [4] have been widely used in bone regeneration studies for years. However, metallic structures have low porosity which limits tissue integration and they are also corrosive and brittle [5] [5]. These properties make metals disadvantageous in scaffolding despite their wide use in the literature [6]. To overcome these drawbacks, scientists investigated the potential of bio-ceramics as bone tissue scaffold [7]. Being a bioactive ceramic, hydroxyapatite (HAP) has taken the lead in bone regeneration studies lately. HAP is highly biocompatible and has an osteoconductive effect [8]. Bioactive and degradable polymeric composite scaffolds are preferred for their ability to stimulate and support bone regeneration to eliminate the frailty disadvantage [9].

The scaffolds degrade at different times depending on the used polymer. It is difficult to determine the rate of degradation of polymeric materials in vivo due to the immune system response to the biomaterial and subsequent fibrous encapsulation. However, cellulose scaffolds have been reported to deteriorate for more than two years [10]. S.S. Liao et al. stated that the in vivo degradation rate of PLA scaffolds containing HAP is higher than in vitro degradation [11]. Xue jun Wang et al. found in vitro degradation of nanohydroxy apatite–PLA scaffolds with and without silica of approximately 12.13% [12]. Zhi Fu and colleagues found that in vivo poly (caprolactone) epoly (ethylene glycol) epoly ($\varepsilon$-caprolactone) scaffolds containing hydroxyapatite was virtually non-degraded after two weeks, with distinct cracks in the scaffolds after four weeks [13]. However, polymeric scaffolds cannot withstand forces. Many researchers have added graphene derivatives into polymers to improve their mechanical strength. In addition to improving physical properties, graphene derivatives can also promote cell proliferation at certain concentrations. Apart from graphene; tricalcium phosphate [14], titanium dioxide [15], zinc oxide [16], cerium oxide [17], cellulose nanocrystals [18] examples of materials used to improve the mechanical strength, swelling behavior, biodegradation, and osteoinduction properties of scaffolds. The scaffolds containing graphene, graphene oxide (GO) and reduced GO have been documented to stimulate tissue regeneration [19]. Graphene-based materials are reported to have different functionality. Therefore, biosensors have been applied to various biomedical and tissue engineering fields such as photothermal therapy, imaging and drug delivery [20]. GO is an oxidized derivative of single-layer graphite. GO has many functional parts on its surface, including hydroxyl, carboxyl, carbonyl

and epoxy groups [21]. This allows it to easily interact with cells and various polymers. Additionally, GO can promote the growth and differentiation of various cell types [22].

In this study HAP supplemented PHBX sponge-like scaffolds are created with incorporating varying concentrations of graphene oxide. Scaffolds were examined morphologically, chemically and biologically and their cytotoxicity, mechanical properties, protein binding efficiencies, degradation profiles and chemical properties were assessed. Bone formation potential of the scaffolds were also determined by gene expression studies after 7, 14 and 28 days of cultivation with MC3T3-E1 cells.

## Material–method

Polyhydroxy butyrate-co-hexanoate (PHBHX) was gifted by Keneka Corporation (Japan). Human serum albumin (HAS), Coomassie blue G250 and MTT [3,4,5-dimethylthiazol-2yl{−2,5-diphenyl-2H-tetrazoliumbromide}] were purchased from SigmaAldrich (USA). MC 3T3 E1 cells were purchased from Sap Institute (Turkey). Alpha MEM medium, fetal bovine serum (FBS), L-glutamine, antibiotic solution, Trypsin–EDTA and phosphate-buffered saline (PBS) were supplied from Gibco (CA).

### Fabrication of the scaffolds

The scaffolds were prepared with a Teflon well plate. The volume of each well was set to 500 µl. PHBHX (6% w/v) solution dissolved in dioxane was mixed in a ratio of 1: 1 (w/w) with HAP (6% w/v) and 6.25 µg or 50 µg graphene oxide solutions prior to pipetting into Teflon plates. Scaffolds were then lyophilized at − 80 °C for two days. After lyophilization, the scaffolds were sterilized with ethylene dioxide and kept at 4 °C [23]. Finally, PHBHX-hydroxyapatite (PHBHX), PHBHX-hydroxyapatite-6.25 µg GO (PHBHXGO1) and PHBHX-hydroxyapatite-50 µg GO (PHBHXGO2) scaffolds were obtained.

### The morphological characterization of the scaffolds

Morphologies of the scaffolds were observed by using a scanning electron microscope at an electron acceleration voltage of 1.5 kV (SEM; Hitachi S-4300, Japan). The scaffolds were coated with the Au—Pl before the examination. After 14 and 28 days of cultivation, morphologies of the cells cultured on the scaffolds were also examined by electron microscopy.

### Chemical characterization of the scaffolds

Attenuated total reflectance–Fourier transform infrared (ATR-FTIR, PerkinElmer) spectroscopy was used for chemical characterization of the scaffolds. The spectra

were collected in the range of 4000–600 $cm^{-1}$, and the resolution was set of values as 16 $cm^{-1}$.

### Water uptake and *in vitro* degradation of the scaffolds

Degradation and water uptake capacity of the scaffolds were determined by the gravimetric method. For this purpose, the scaffolds ($n = 3$) were put into pH 7.4 PBS and kept at 37 °C for 1 h. The wet weight of the scaffolds was then weighed and kept at 37 °C. The wet weights of the scaffolds were weighed weekly for eight weeks.

### Compression test of the scaffolds

Mechanical properties of the scaffolds were determined by an axial compression test via a dynamic mechanic test machine (H25K-S Tinius Oslen, USA). The preload value was 6 MPa, and the test speed was 1.5 mm/min [24].

### Albumin binding assay

Human serum albumin binding properties of the scaffolds were determined. For this purpose, the scaffolds were put into 500 µg/ml human serum albumin solution and kept at 37 °C for two hours. After incubation, the scaffolds were gently washed with PBS and poured into a PBS solution containing 0.5% TritonX100. The scaffolds were incubated for 30 min at 37 °C. The amount of protein remaining in the aqueous phase was then measured with Coomassie blue buffer. To prepare Coomassie blue G250buffer, 10 mg Coomassie blue G250 dye was dissolved in 5 ml ethanol, 85 ml water and 10 ml phosphoric acid [25].

### Cell culture studies

MC 3T3 cells were cultured in the alpha MEM medium supplemented with 10% FCS. The cells were maintained at 37 °C in a humidified atmosphere of 5% $CO_2$. GO was sterilized in autoclave. Then, the cytotoxicity of GO in different concentrations on MC3T3 cells was determined via XTT method. According to the results, two concentration of GO was determined and added to the PHBHX scaffolds.

To determine the cell proliferation rate on the scaffolds, MC3T3 E1 cells were collected in FCS and seeded onto the scaffolds. The medium with cells was added onto the scaffolds, and after incubation of 7, 14 and 28 days, the cell concentration was determined by the XTT method, and also, the cells cultured onto the scaffolds were investigated by SEM images.

Before the SEM examinations, scaffolds were washed with PBS and fixed with 4% paraformaldehyde solution at 4 °C for 30 min. The scaffolds were coated with gold and evaluated by SEM (Tescan, GAIA 3, Czechia).

### Gene expression studies

Cells were harvested from scaffolds after 7, 14 and 28 days of incubation. RNA isolation was performed according to kit protocol (Zymo Research Quick RNA Miniprep kit, USA). Isolated RNA was controlled with NanoDrop 2000 Spectrophotometer (Thermo Scientific, USA) prior to cDNA synthesis, and 100 ng of RNA was used per sample for following step. cDNA synthesis was performed using Revert Aid First Strand cDNA Synthesis kit (Thermo Scientific, USA). qPCR was performed via Quant Studio 5 System (Applied Biosystems, USA). Primers used are given in the Table 1, and ACTB was used as housekeeping gene. Each sample was studied in three replicates. Results were analyzed with comparative Ct method.

### Statistical analysis

Multiple comparisons of the groups were made with a Tukey test after one-way analysis of variance. A statistical significance level of $P < 0.05$ was considered significant. All data were showed as the mean value ± standard deviation. GraphPad Prism 6.0 was used for statistical analysis of results relative gene expression. One-way ANOVA and t-test were performed. Results are summarized with asterisks on relative gene expression graph: "$p > 0.05$" shown as *ns*, "$P \leq 0.05$" shown as *, "$p \leq 0.01$" shown as **, "$P \leq 0.001$" as *** and "$P \leq 0.0001$" as ****.

## Results and discussion

Regeneration of bone tissue is a medical challenge by means of morphology and functionality. The body has the capacity to regenerate lost alveolar bone when appropriate conditions occur, which is enhanced by implanting bone grafts to the damaged bone to accelerate the healing of missing or lost alveolar bone. Functional tissue engineering products offer new opportunities for bone tissue regeneration. In this study, graphene oxide and HAP were used to enhance capability of PHBHX scaffolds for bone formation. First, the cytotoxicity of graphene oxide at different concentrations on MC3T3 cells was determined. According to the results of cytotoxicity studies, two different concentrations of graphene oxide (low and high) were

**Table 1** List of primers used in gene expression studies

| | Forward primer (5′-3′) | Reverse primer (5′-3′) |
|---|---|---|
| ACTB | GTGCTATGTTGCCCTAGACTTCG | ATGCCACAGGATTCCATACCC |
| COL1A1 | AGATGTGCCACTCTGACTCC | ACTGACCTGTCTCCATGT |
| OCN | TTTCTGCTCACTCTGCTG | TATTGCCCTCCTGCTAG |
| OPN | CTCCAATCGTCCCTACGG | TCCTTAGACTCGACTC |
| RUNX2 | GCATGGCCAAGAAGACA | TCGGGTTTCCACGTTAGC |

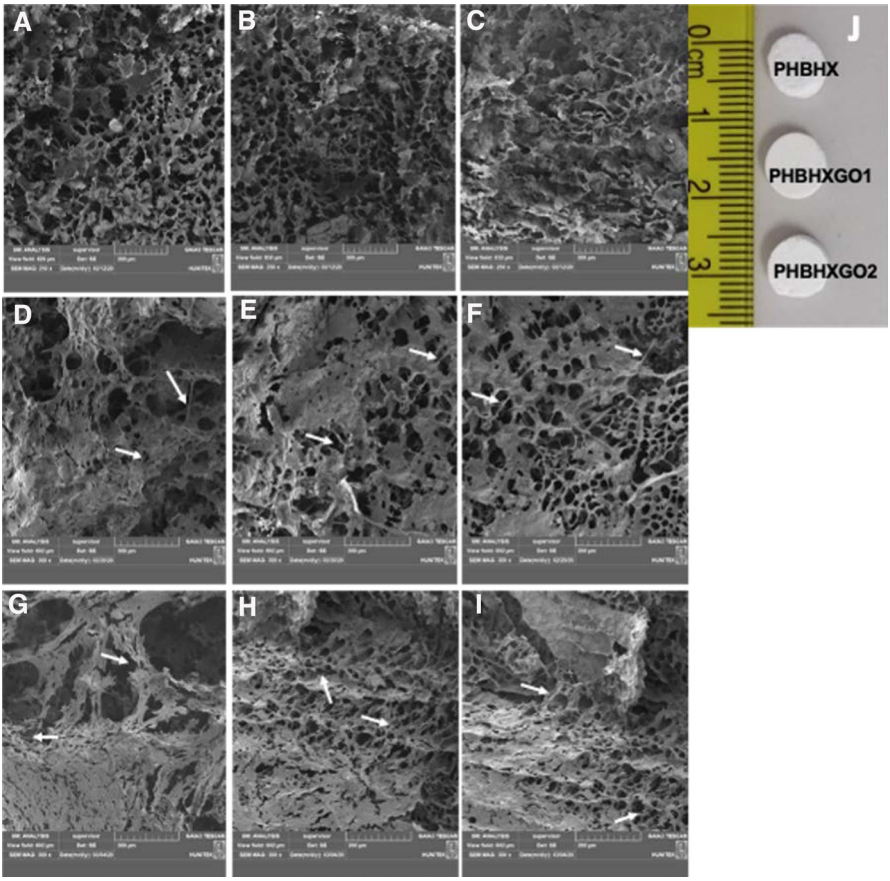


**Fig. 1** SEM photographs of the PHBHX **a**, PHBHXGO1 **b**, PHBHXGO2 **c** scaffolds. 14th day, SEM photographs of MC3T3 E1 cells on the PHBHX **d**, PHBHXGO1 **e**, PHBHXGO2 **f** scaffolds. 28th day, SEM photographs of MC3T3 E1 cells cultured on the PHBHX **g**, PHBHXGO1 **h**, PHBHXGO2 **i** scaffolds. Macroscopic photographs of the scaffolds **j**. Arrows indicate MC3T3 E2 cell pseudopods

determined, and at these concentrations, graphene oxide was loaded on the scaffolds. Macroscopic and SEM photographs of the scaffolds was given in Fig. 1.

The structure of adequate porosity provides an opportunity for cell migration and proliferation [26]. According to the SEM images, random, macron size porous areas were observed in the scaffolds with and without GO. Pore diameters of the scaffolds were measured with SEM photographs using the ImageJ program. Pore diameters of PHBHX (Fig. 1a), PHBHXGO1 (Fig. 1b) and PHBHXGO2 (Fig. 1c) were measured as $76.39 \pm 13.21$, $59.42 \pm 10.1$ and $48.96 \pm 13.52$ µm, respectively. As a result of the ImageJ measurements (Fig. 1j), it was observed that although the inclusion of GO decreased porosity ($P < 0.05$), there were no significant differences between PHBHXGO1 and PHBHXGO2 scaffolds ($P > 0.05$). There are controversial results in the literature about how scaffold porosity is affected with GO inclusion. Wang W

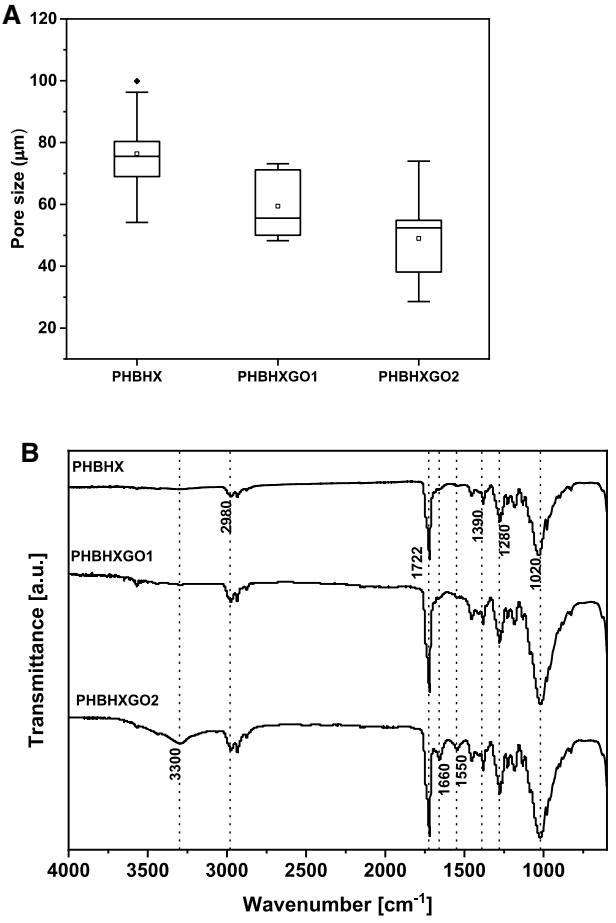


**Fig. 2** Pore size **a** and ATR-FTIR spectra **b** of PHBHX, PHBHXGO1 and PHBHXGO2 scaffolds

and colleagues expressed that GO addition slightly increased the porosity of scaffolds [27]. However, Norahan MH and colleagues determined that the inclusion of GO decreased porosity [28]. We found GO decreased the scaffold porosity, but its varying amounts did not change the overall morphology significantly (Fig. 2a).

## Chemical characterization of the scaffolds

Chemical characterization of the scaffolds was performed by ATR-FTIR. ATR-FTIR spectrum of the scaffolds is presented in Fig. 2b. The peaks at around 3000 $cm^{-1}$ represent the C–H stretching vibration of aliphatic groups in graphene oxide [29] and PHBHX. A wide –OH peak of graphene oxide was seen at 3300 $cm^{-1}$. C=O band in PHBHX and graphene oxide was seen at 1722 $cm^{-1}$. At 1600 cm-1, stretching band of COO– in graphene oxide was seen and the band was seen very weak in

the PHBHX spectrum [30]. –CH bending peak of PHBHX and graphene oxide was observed at 1390 $cm^{-1}$. The shark peak at 1280 $cm^{-1}$ denotes C–O–C stretching in graphene oxide and PHBHX and at 1020 $cm^{-1}$ corresponds to the vibrational of the C–O group in PHBHX and graphene oxide.

### Swelling and in vitro degradation properties of the scaffolds

The swelling and in vitro degradation properties of the scaffolds were determined by the gravimetric method. The swelling rate is associated with nutrient and waste transport. Therefore, it is an important parameter in tissue engineering [31]. Figure 3a represents the swelling ratio of the scaffolds. The swelling ratio

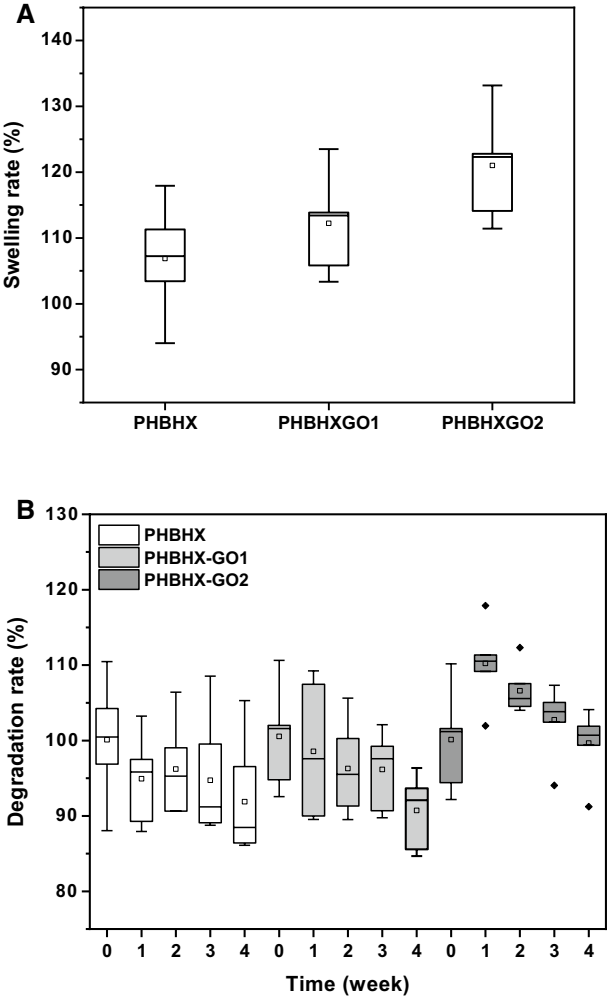


**Fig. 3** Swelling rate **a** and degradation rate **b** of the PHBHX, PHBHXGO1, PHBHXGO2 scaffolds

of the PHBHX, PHBHXGO1 and the PHBHXGO2 scaffolds was calculated to be 106.86 ± 8.29%, 112.22 ± 7.1% and 121.01 ± 7.6%, respectively. These results indicate the hydrophilic properties of GO and mixing with PHBHX modifies the scaffolds to be more hydrophilic. Francolini I and colleagues indicated that GO (exfoliated and concentration of 0.3%) increased swelling ration of the scaffold; however, increasing GO concentration decreased swelling ration because of hydrophobic C=C bounds of graphene oxide [32].

Degradation rate is an important feature of bone substitutes. A scaffold to degrade within a reasonable time frame can lead to space for new bone formation. The fast or slow degradation rate could lead to bone defects in the operation area. It is known that degradation rate of hydroxyapatite is slower than beta-tricalcium phosphate [33]. Zhang L and colleagues demonstrated that biphasic calcium phosphate and hydroxyapatite better stimulated differentiation of mesenchymal cells than beta-tricalcium phosphate [34]. The weight loss of the PHBHX, PHBHXGO1 and PHBHXGO2 scaffold after 4 weeks was determined about 8.11 ± 0.76%, 9.26 ± 0.46 and 3.3 ± 0.44, respectively (Fig. 3b). These results indicate the GO modification of the scaffolds decreased degradation rate. Shin Y.C. and colleagues suggested that because of the interfacial interaction of the molecules, degradation of PLGA-GO-RGD membrane was slower than PLGA-GO and bare PLGA nanomembrane [35] RGD peptide and graphene oxide co-functionalized PLGA nanofiber scaffolds for vascular tissue engineering. In parallel with our results, Khan M.U.A., and colleagues reported that the rate of degradation of the scaffold was slower as the graphene oxide concentration increased [36]. Seyedsalehi A. and colleagues reported similar results [37].

## Compression test of the scaffolds

The mechanical property of the scaffolds was determined and presented as compressive strength in Fig. 4a. The compressive strength at 10% strain of the PHBHX, PHBHXGO1 and PHBHXGO2 scaffolds was observed to be 0.86, 0.97 and 1.29 MPa, respectively. The compressive strength at 50% strain of the PHBHX, PHBHXGO1 and PHBHXGO2 scaffolds was observed to be 4.14, 4.64 and 6.18 MPa, respectively. The results indicated that increasing GO concentration increased compressive stress. Purohit S.D. and colleagues expressed that adding GO and HAP increased compressive stress value of gelatin scaffolds. They also indicated that it may be intermolecular physical/chemical cross-linking of GO and polymer [38]. Shuai C. and colleagues prepared polyvinylidene fluoride scaffolds, added 0.1, 0.3 and 0.5% GO to the composite. They indicated that adding 0.1 and 0.3% GO increased the compression stress of the scaffolds, but 0.5% GO decreased [39]. Meanwhile, Zimba BL and colleagues prepared collagen, hydroxyapatite and graphene oxide scaffold and expressed that compressive stress pressure stress is proportional to the amount of collagen [40]. In line with

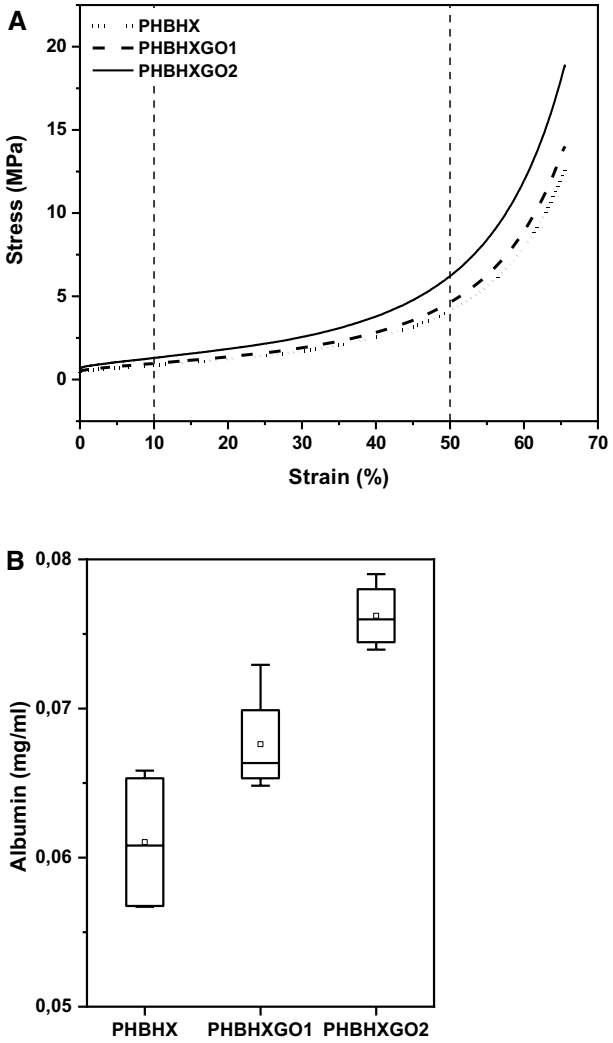


**Fig. 4** Compression test **a** and albumin absorption **b** of the PHBHX, PHBHXGO1 and PHBHXGO2 scaffolds

our results, Zhang Y and colleagues expressed that GO increased compression stress and degreased degradation ratio of scaffolds [41].

## Albumin binding assay

Protein binding on a biomaterial mediates cell adhesion and consequently cell proliferation on scaffolds. Therefore, the determination of the amount of adherent protein is vital to predict in vivo efficiency of a scaffold [42]. The results of the HSA adherence test are presented in Fig. 4b. Reversible HAS

binding of the PHBHX, PHBHXGO1 and PHBHXGO2 scaffolds were measured as $61.04 \pm 4.96$, $67.60 \pm 3.64$ and $76.22 \pm 2.22$ µg, respectively. According to the results, the incubation of the scaffolds in a protein solution (0.5 mg/mL) caused protein attachment on the surface of the scaffolds. It was observed that adding GO to the PHBHX scaffolds enhanced protein binding ($P < 0.05$), and also, it was determined that increasing GO concentrations increased the HSA amount adherent to the surface ($P < 0.05$). It is concluded that GO addition increases surface polarity due to its functional groups, promoting protein binding. Saravanan S and

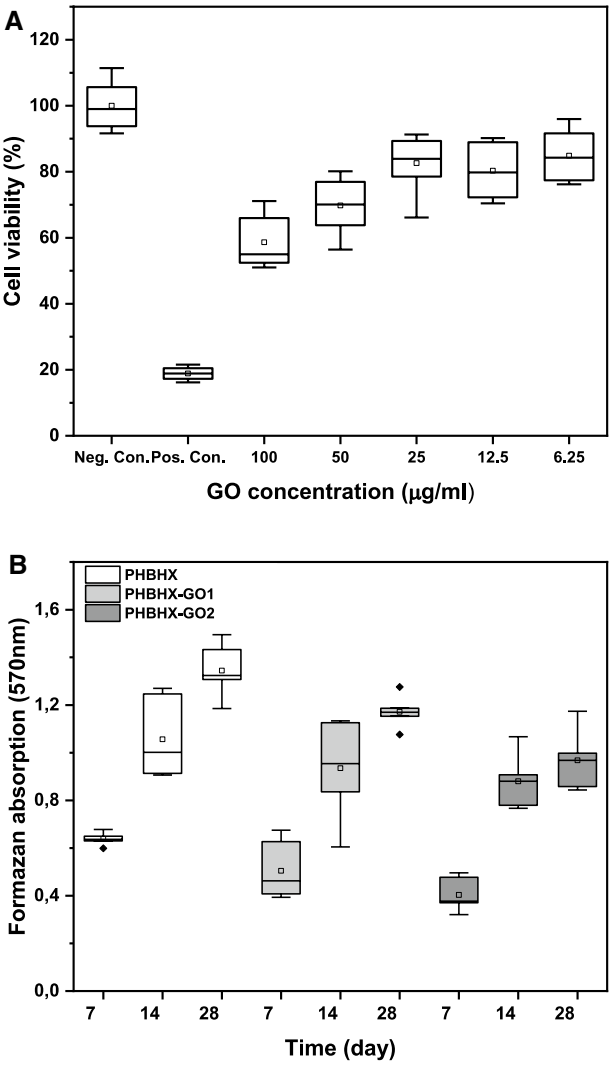


**Fig. 5** Cytotoxicity of GO **a** and formazan absorption of MC3T3 cells, cultured on the PHBHX, PHBHXGO1, PHBHXGO2 scaffolds **b**

colleagues also demonstrated that the inclusion of GO increased protein binding on scaffolds in line with our findings [43].

### Cell culture studies

The toxicity of GO is related to oxygen content. High oxygen concentration increases reactive oxygen species, and reactive oxygen species are cytotoxic [44]. Therefore, before the scaffold fabrication, cytotoxicity of the GO (100, 50, 25, 12.5, 6.25 µg/ml) on MC3T3 E1 cells was determined by XTT test (Fig. 5a). The XTT test result indicated that 100, 50 and 6.25 µg/ml GO cytotoxicity was found as $41.37 \pm 7.9$, $30.23 \pm 8.17$ and $15.13 \pm 7.82$, respectively. Regarding the XTT results, high (50 µg/ml) and low (6.25 µg/ml) concentrations of the GO were decided for the addition to PHBHX bone scaffolds.

MC3T3 cells were cultured on the scaffolds, and the cell proliferated on the scaffolds was determined by the XTT test. When the groups were compared within, it was observed that cell proliferation increased in all groups ($P < 0.05$). However, the highest formazan absorbance was measured in PHBHX scaffolds, and the difference in formazan concentration was parallel on day 28 ($P < 0.05$). In contrast to our finding, Norahan MH and colleagues indicated that the collagen scaffolds containing 400 µg/ml GO increased endothelial cell concentration [28]. Also, Nishida E. and colleagues reported that MC3T3 cell proliferation on collagen scaffolds containing 1 µg/mL GO was 1.6-fold greater than that of control [45].

SEM images of the cells 14 and 28 days cultured on the scaffolds were taken. According to the SEM images, it was observed that cells were well spread on all scaffolds, and fine filamentous extension linked to the scaffold surface and each other cells [46].

### Gene expression studies

Osteoblastic differentiation of MC3T3-E1 cells was examined after cultivation with PHBHX, PHBHXGO1 and PHBHXGO2 scaffolds for 7, 14 and 28 days. Relative mRNA levels of RUNX2, COL1A1, OCN and OPN genes were investigated. Bone formation occurs in three temporal phases as proliferation, matrix maturation and mineralization. RUNX2 is an early-stage differentiation protein, which is shown to be increased on day 7 remarkably, with the addition of GO in our study ($p \leq 0.0001$) (Fig. 6a). The increase in RUNX2 gene expression continued on day 14 and day 28, although it seemed to be in a slower rate in day 28 ($P \leq 0.001$). OCN, OPN genes are considered as late-stage gene expression markers of bone differentiation. On day 28, mRNA level of OPN was increased significantly in cells on PHBHXGO2 scaffolds compared to PHBHX scaffolds ($P \leq 0.001$). Significant increase in OPN mRNA levels was also observed comparing PHBHXGO1 and PHBHXGO2 scaffolds on each day of cultivation ($P \leq 0.05$), showing higher amounts of GO addition lead to enhanced gene expression levels (Fig. 6b). For OCN gene expression levels, comparing PHBHX and PHBHXGO2 scaffolds a statistically important increase

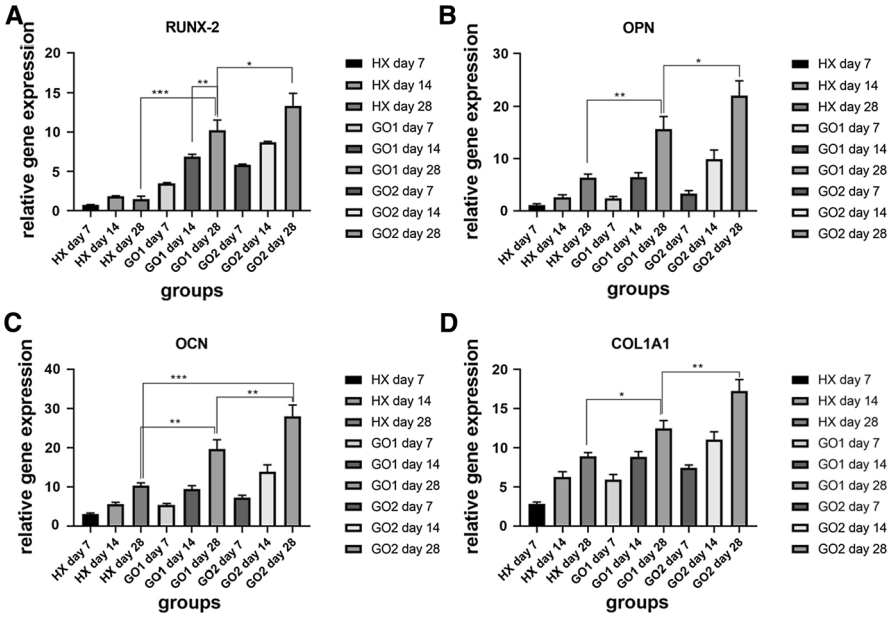


**Fig. 6** Relative gene expression levels of MC3T3 cells cultured on the PHBHX, PHBHXGO1, PHBHXGO2 scaffolds, **a** RUNX2 gene expression levels on day 7, 14 and 28 of cultivation, **b** OPN gene expression levels on day 7, 14 and 28 of cultivation, **c** OCN gene expression levels on day 7, 14 and 28 of cultivation, **d** COL1A1 gene expression levels on day 7, 14 and 28 of cultivation

was also determined on day 28 ($p \leq 0.001$), as well as on days 7 ($P \leq 0.0001$) and 14 ($P \leq 0.001$) of cultivations, clearly demonstrating the efficiency of GO incorporation into PHBHX scaffolds for bone formation (Fig. 6c). COL1A1 gene expression levels were also examined as collagen 1 being the most abundant bone protein. Results showed a significant increase in COL1A1 mRNA levels between PHBHX and PHBHXGO2 scaffolds on days 14 and 28 ($P \leq 0.001$) of cell culture. Comparing the gene expression levels of PHBHXGO1 and PHBHXGO2 scaffolds, it is showed that COL1A1 levels were increased with increasing GO amounts significantly in day 7 and 14 ($P \leq 0.05$) and 28 ($P \leq 0.01$) (Fig. 6d). Overall, increasing GO amounts increased the gene expression levels significantly for all genes examined, demonstrating the potential of graphene oxide for bone differentiation.

## Conclusions

Graphene oxide-containing polymeric scaffolds are being investigated for bone tissue engineering. There are many articles related to scaffold containing graphene oxide for bone tissue engineering [47]. Meanwhile, in articles, the graphene oxide concentration used is very different. Therefore, in the presented study, primarily cytotoxicity of graphene oxide was determined depending on the concentration. The highest GO concentration which is not cytotoxic for MC3T3

cells was determined. And then as a low concentration, non-cytotoxic graphene oxide concentration was determined. PHBHX scaffolds containing low and high concentrations of GO were fabricated and characterized. According to the results, GO increased water uptake, albumin adsorption and also ACTB, COL1A1, OCN, OPN, RUNX2 gene expression. Meanwhile, MC3T3 cell concentrations cultured on the PHBHXGO1 and PHBHXGO2 were found low than PHBHX scaffolds. It is suggested that GO containing scaffolds needed more comprehensive examination.

**Acknowledgements** This study was conducted at Hacettepe University Advanced Technologies Application and Research Center (HUNITEK) and not supported by any institution. There is no conflict between the authors.

**Funding** The study was not supported by any institution or organization.

## References

1. Böttcher-Haberzeth S, Biedermann T, Reichmann E (2010) Tissue engineering of skin. Burns 36(4):450–460
2. Bártolo P et al (2009) Biomanufacturing for tissue engineering: present and future trends. Virtual Phys Prototyp 4(4):203–216
3. Lantada AD, Morgado PL (2012) Rapid prototyping for biomedical engineering: current capabilities and challenges. Annu Rev Biomed Eng 14:73–96
4. Yazdimamaghani M et al (2015) Significant degradability enhancement in multilayer coating of polycaprolactone-bioactive glass/gelatin-bioactive glass on magnesium scaffold for tissue engineering applications. Appl Surf Sci 338:137–145
5. Ghassemi T et al (2018) Current concepts in scaffolding for bone tissue engineering. Arch Bone Jt Surg 6(2):90
6. Liu Y et al (2014) Hydroxyapatite/graphene-nanosheet composite coatings deposited by vacuum cold spraying for biomedical applications: inherited nanostructures and enhanced properties. Carbon 67:250–259
7. Hench LL (1991) Bioceramics: from concept to clinic. J Am Ceram Soc 74(7):1487–1510
8. Wang L et al (2010) Osteogenesis and angiogenesis of tissue-engineered bone constructed by prevascularized β-tricalcium phosphate scaffold and mesenchymal stem cells. Biomaterials 31(36):9452–9461
9. Razavi M et al (2014) In vivo study of nanostructured diopside (CaMgSi2O6) coating on magnesium alloy as biodegradable orthopedic implants. Appl Surf Sci 313:60–66
10. Purohit SD et al (2019) Development of a nanocomposite scaffold of gelatin–alginate–graphene oxide for bone tissue engineering. Int J Biol Macromol 133:592–602
11. Liao S, Cui F (2004) In vitro and in vivo degradation of mineralized collagen-based composite scaffold: nanohydroxyapatite/collagen/poly (L-lactide). Tissue Eng 10(1–2):73–80
12. Wang X, Song G, Lou T (2010) Fabrication and characterization of nano-composite scaffold of PLLA/silane modified hydroxyapatite. Med Eng Phys 32(4):391–397
13. Fu S et al (2012) In vivo biocompatibility and osteogenesis of electrospun poly (ε-caprolactone)–poly (ethylene glycol)–poly (ε-caprolactone)/nano-hydroxyapatite composite scaffold. Biomaterials 33(33):8363–8371
14. Sulaiman SB et al (2013) Tricalcium phosphate/hydroxyapatite (TCP-HA) bone scaffold as potential candidate for the formation of tissue engineered bone. Indian J Med Res 137(6):1093
15. Abou Neel E, Knowles J (2008) Physical and biocompatibility studies of novel titanium dioxide doped phosphate-based glasses for bone tissue engineering applications. J Mater Sci: Mater Med 19(1):377–386

16. Feng P et al (2014) Characterization of mechanical and biological properties of 3-D scaffolds reinforced with zinc oxide for bone tissue engineering. PloS one 9(1):e87755
17. Xiang J et al (2016) Cerium oxide nanoparticle modified scaffold interface enhances vascularization of bone grafts by activating calcium channel of mesenchymal stem cells. ACS Appl Mater Interfaces 8(7):4489–4499
18. Zhang C et al (2015) Incorporation of poly (ethylene glycol) grafted cellulose nanocrystals in poly (lactic acid) electrospun nanocomposite fibers as potential scaffolds for bone tissue engineering. Mater Sci Eng, C 49:463–471
19. Shin YC et al (2015) Stimulating effect of graphene oxide on myogenesis of C2C12 myoblasts on RGD peptide-decorated PLGA nanofiber matrices. J Biol Eng 9(1):1–10
20. Ding X, Liu H, Fan Y (2015) Graphene-based materials in regenerative medicine. Adv Healthc Mater 4(10):1451–1468
21. Shin YC et al (2017) Graphene oxide-incorporated PLGA-collagen fibrous matrices as biomimetic scaffolds for vascular smooth muscle cells. Sci Adv Mater 9(2):232–237
22. Zhou X et al (2017) 3D bioprinted graphene oxide-incorporated matrix for promoting chondrogenic differentiation of human bone marrow mesenchymal stem cells. Carbon 116:615–624
23. Eltom A, Zhong G, Muhammad A (2019) Scaffold techniques and designs in tissue engineering functions and purposes: a review. Adv Mater Sci Eng 2019:1–13
24. Gregor A et al (2017) Designing of PLA scaffolds for bone tissue replacement fabricated by ordinary commercial 3D printer. J Biol Eng 11(1):1–21
25. Nair A et al (2010) Novel polymeric scaffolds using protein microbubbles as porogen and growth factor carriers. Tissue Eng Part C Methods 16(1):23–32
26. Karageorgiou V, Kaplan D (2005) Porosity of 3D biomaterial scaffolds and osteogenesis. Biomaterials 26(27):5474–5491
27. Wang W et al (2019) Mesoporous bioactive glass combined with graphene oxide scaffolds for bone repair. Int J Biol Sci 15(10):2156
28. Norahan MH et al (2019) Electroactive cardiac patch containing reduced graphene oxide with potential antibacterial properties. Mater Sci Eng: C 104:109921
29. Cao N, Zhang Y (2015) Study of reduced graphene oxide preparation by Hummers' method and related characterization. J Nanomater 2015:1–5
30. Shen L et al (2015) Production of poly (3-hydroxybutyrate-co-3-hydroxyhexanoate) from excess activated sludge as a promising substitute of pure culture. Biores Technol 189:236–242
31. Kavya K et al (2013) Fabrication and characterization of chitosan/gelatin/nSiO2 composite scaffold for bone tissue engineering. Int J Biol Macromol 59:255–263
32. Francolini I et al (2019) Graphene oxide oxygen content affects physical and biological properties of scaffolds based on chitosan/graphene oxide conjugates. Materials 12(7):1142
33. Newe C et al (2012) Static and dynamic degradation of sintered calcium phosphate ceramics. In: Key engineering materials, vol 493–494. Trans Tech Publ, pp 861–865
34. Zhang L et al (2009) Porous hydroxyapatite and biphasic calcium phosphate ceramics promote ectopic osteoblast differentiation from mesenchymal stem cells. Sci Technol Adv Mater 10(2):025003
35. Shin YC et al (2017) RGD peptide and graphene oxide co-functionalized PLGA nanofiber scaffolds for vascular tissue engineering. Regen Biomater 4(3):159–166
36. Khan MUA et al (2021) Synthesis and characterization of silver-coated polymeric scaffolds for bone tissue engineering: antibacterial and in vitro evaluation of cytotoxicity and biocompatibility. ACS Omega 6(6):4335–4346
37. Seyedsalehi A et al (2020) Fabrication and characterization of mechanically competent 3D printed polycaprolactone-reduced graphene oxide scaffolds. Sci Rep 10(1):1–14
38. Purohit SD et al (2020) Fabrication of graphene oxide and nanohydroxyapatite reinforced gelatin–alginate nanocomposite scaffold for bone tissue regeneration. Front Mater 7:1–10
39. Shuai C et al (2020) Graphene oxide assists polyvinylidene fluoride scaffold to reconstruct electrical microenvironment of bone tissue. Mater Des 190:108564
40. Zimba BL et al (2019) Preparation and characterizations of three-dimensional porous collagen/graphene oxide/hydroxyapatite nanocomposite scaffolds for bone tissue engineering. Open Sci J. https://doi.org/10.23954/osj.v4i1.2123
41. Zhang Y et al (2019) Fabrication and application of novel porous scaffold in situ-loaded graphene oxide and osteogenic peptide by cryogenic 3D printing for repairing critical-sized bone defect. Molecules 24(9):1669

42. E Silva Filho FC, Menezes GC (2004) Osteoblasts attachment and adhesion: how bone cells fit fibronectin-coated surfaces. Mater Sci Eng: C 24(5):637–641
43. Saravanan S et al (2017) Scaffolds containing chitosan, gelatin and graphene oxide for bone tissue regeneration in vitro and in vivo. Int J Biol Macromol 104:1975–1985
44. Bengtson S et al (2016) No cytotoxicity or genotoxicity of graphene and graphene oxide in murine lung epithelial FE1 cells in vitro. Environ Mol Mutagen 57(6):469–482
45. Nishida E et al (2016) Graphene oxide scaffold accelerates cellular proliferative response and alveolar bone healing of tooth extraction socket. Int J Nanomed 11:2265
46. Wang JK et al (2015) Polymer-enriched 3D graphene foams for biomedical applications. ACS Appl Mater Interfaces 7(15):8275–8283
47. Prasadh S, Suresh S, Wong R (2018) Osteogenic potential of graphene in bone tissue engineering scaffolds. Materials 11(8):1430